Original Article
Clinical implications of PD-L1 expression and pathway-related molecular subtypes in advanced Asian colorectal cancer patients

Qingqing Qiu[1*], Dan Tan[1*], Qiaofeng Chen[1*], Ru Zhou[1], Xiaokai Zhao[3,4], Wei Wen[3,4], Pengmin Yang[3,4], Jieyi Li[3,4], Ziying Gong[3,4], Daoyun Zhang[3,4], Mingliang Wang[1,2*]

[1]Department of General Surgery, RuiJin Hospital Lu Wan Branch, Shanghai Jiaotong University School of Medicine, Shanghai 200020, China; [2]Department of General Surgery, RuiJin Hospital, Shanghai Jiaotong University School of Medicine, Shanghai 200025, China; [3]Jiaxing Key Laboratory of Precision Medicine and Companion Diagnostics, Jiaxing Yunying Medical Inspection Co., Ltd., Jiaxing 314000, Zhejiang, China; [4]Department of R&D, Zhejiang Yunying Medical Technology Co., Ltd., Jiaxing 314000, Zhejiang, China. *Equal contributors and co-first authors.

Abstract: The expression level of PD-L1 does not accurately predict the prognosis of advanced colorectal cancer (CRC) patients, but it still reflects the tumor microenvironment to some extent. By stratifying PD-L1 status, gene subtypes in PD-L1 positivity-related pathological pathways were analyzed for their relationship to MSI or TMB to provide more individualized treatment options for CRCs. A total of 752 advanced CRCs were included, and their genomic variance was measured by a targeted next generation sequencing panel in this study. MSI and TMB were both measured by NGS, while PD-L1 expression level was measured using the PD-L1 colon 22C3 pharmDx kit. We found RTK/RAS pathway was positively related to high PD-L1 expression, with *BRAF V600E* and most *KRAS* mutations (G12 and G13) subtypes showing a significant correlation. Conversely, the Wnt and p53 pathways were negatively related to high PD-L1 expression, with *APC* C-terminal alterations and other non-inactivation mutations in *TP53* making a primary contribution with significant statistical significance. Major subtypes showing a significantly higher proportion of TMB-H or MSI-H were irrespective of PD-L1 status. These findings demonstrate pathological pathways associated with high PD-L1 expression, suggesting that pathway-induced oncogenic constructive PD-L1 upregulation may be the reason for the corresponding patients' primary resistance to immune checkpoint inhibitors (ICIs), rather than a lack of pre-existing immune responses.

Keywords: TMB, MSI, programmed death-ligand 1 (PD-L1), advanced colorectal cancer (CRC)

Introduction

Immune checkpoint inhibitors (ICIs) have achieved dazzling clinical efficacy in various advanced solid tumors, providing more treatment options for advanced patients [1]. Nevertheless, Pembrolizumab, one type of PD-1 ICIs, was only recently approved by the FDA for the first-line treatment of mismatch-repair-deficient (dMMR)/microsatellite instability-high (MSI-H) metastatic colorectal cancer (mCRC) patients [2]. Given the unclear response mechanism of patients to immunotherapies, multiple clinical trials, including monotherapy [2, 3], combination of ICIs [4], radiotherapy [5], MEK inhibitor [6, 7] and anti-angiogenic agents [8], are under-

way to identify more suitable treatment regimens and prognostic biomarkers for different subtypes of CRC. Generally accepted immunotherapy biomarkers for colorectal cancer include microsatellite instability (MSI) [9], tumor mutation burden (TMB) [10, 11], and *POLE* gene mutation [12]. The proportion of *POLE* gene mutations in the Asian patient population is relatively small [13]. In comparison, MSI and TMB testing provide a distinct advantage in personalized treatments for Asian patients.

The rate of MSI-H is relatively low in mCRC, at about 5% [14-16], while the proportion of TMB high level is slightly higher with a positivity rate about 10% at a cutoff of 10 muts/Mb [17, 18].

Consequently, only a small number of advanced CRCs can benefit from immunotherapy, and other potential biomarkers remain to be explored. In comparison to these two biomarkers, PD-L1 status, with a positivity rate about 10% in CRCs [19], has received inconsistent conclusions regarding its prognostic effect and its ability to predict response to ICIs [20-22]. Although PD-L1 status cannot serve as an individual biomarker for predicting the efficacy of immunotherapy in clinical applications [23, 24], it is still closely associated with an active immune microenvironment in some pathways [25, 26]. Additionally, the high heterogeneity of CRCs at the genomic level is also one of the reasons for the significant difference in curative effect, suggesting that gene molecular typing may play an important role in the clinical treatment of advanced CRCs. Moreover, meta-analyses have also linked PD-L1 expression to a poor prognosis in colorectal cancer [27, 28]. Our study aims to compare gene mutation profiles between PD-L1 positive and negative groups and analyze gene enrichment related to tumor signaling pathways. This exploration seeks to uncover potential mechanisms associated with a poor prognosis. Furthermore, we conducted a detailed stratified analysis of key genes related to PD-L1 expression, along with assessments of TMB and MSI. This comprehensive approach helps identify patient subgroups that may benefit from targeted therapy, immunotherapy or a combination of both, offering novel insights into precision treatment for colorectal cancer.

Methods

Patient and sample characteristics

A total of 809 patients with stage IV advanced colorectal cancer were enrolled in this study at Ruijin Hospital from January 2021 to May 2023. Samples lacking paired blood, without pathological confirming of CRC, and with a tumor content of less than 20% were all excluded, resulting in 752 samples from 752 patients being included. Clinical data, including age and gender, were obtained from medical records. Written informed consent was obtained from all participants, and this study was approved by the institutional review board of our hospital (LWEC2020010).

DNA extraction and library construction

The extraction and purification of blood DNA and tissue DNA are implemented by using the human blood genome DNA extraction kit (Shanghai YunYing) and the human tissue DNA extraction kit (Shanghai YunYing), respectively. NanoDrop2000 (Thermo Fisher Scientific, Waltham, MA, USA) was applied to evaluate the contamination and purity of samples, followed by a storage at -20°C before use. The VAHTS Universal DNA Library Prep Kit for Illumina was used for library preparation. Shanghai YunYing's optimized probes, which target the exons and some introns of 639 genes related to cancer (Table S4), were applied. Targeted-sequencing was performed on the NextSeq500 platform (Illumina, Carlsbad, CA, USA) strictly following the manufacturer's protocols.

NGS-based assay and bioinformatical analysis

FastQC software (version 0.11.2) was used for the screening of FASTQ files. Customized Python scripts were conducted to remove the sequence from adaptor or with a quality score below 30. Referring on the human genome GRCh37/hg19, clean reads were mapped by the Burrows-Wheeler Aligner (BWA, version 0.7.7), resulting in corresponding bam files which were realigned and recalibrated by GATK3.5. Picard MarkDuplicates (version 1.35) was used to remove duplicate sequences and reduce potential polymerase chain reaction bias. Single nucleotide variations (SNVs) were detected by VarScan (version 2.3.2) following the criteria: (1) Total reads depth was more than 500; (2) Mutated reads frequency was higher than 1%. Insertion of deletion (indel) was detected by Pindel (version 0.2.5b8) with default parameters. FACTERA (version 1.4.4) was applied to identify structure variation using default parameters.

Mutation difference of somatic SNVs and Indels were compared between tumor samples and matched normal samples by MuTect (version 1.1.4), followed by functional annotations using Verscan2 (version 2.3.9). The number of all somatic, coding, base substitution and indel mutations per megabase were used to calculate tumor mutation burden (TMB). Thus, the TMB per megabase was calculated by the quo-

Table 1. Patient characteristics

Characteristics	PD-L1 positive No. (%) (n=127)	PD-L1 negative No. (%) (n=625)	[a]P value
Total	127 (100)	625 (100)	
Gender			
Male	70 (55.12)	408 (65.28)	0.04
Female	57 (44.88)	217 (34.72)	
Age at diagnosis in years			
< 60	63 (49.61)	275 (44.00)	0.3
≥ 60	64 (50.39)	350 (56.00)	
MSI state			
MSI-H	15 (11.81)	25 (4.00)	0.002
Non MSI-H (MSS and MSI-L)	112 (88.19)	600 (96.00)	
Tumor mutation burden status			
TMB-H (≥ 10 muts/Mb)	20 (15.75)	63 (10.08)	0.09
TMB-L (< 10 muts/Mb)	107 (81.89)	562 (89.92)	

[a]P value are tested by Fisher's exact Test.

tient of the counted total mutation number divided by the size of the coding region of the targeted territory (1.1 Mb of coding genome).

MSIsensor [29], a software tool for quantifying MSI in genome sequencing data using tumor samples with or without paired normal ones, were applied to calculate the MSI score of all samples with default parameters. The MSI score was defined as the percentage of unstable microsatellites in all used microsatellites. At least 20 spanning reads and single-nucleotide mutations would be included in each microsatellite site.

PD-L1 expression level was measured by immunohistochemical (IHC) method and assessed by experienced pathologists. According to the PD-L1 IHC 22C3 pharmDx package insert, TPS was calculated to determine the expression level of PD-L1. Briefly, TPS was defined as the number of viable tumor cells displaying partial of complete membrane staining of PD-L1 which is divided by the total number of viable tumor cells and then multiplied by 100%. The TPS value which is 1% or more than 1% is defined as PD-L1 positivity and that less than 1% is grouped as PD-L1 negativity.

Mutations in *APC* are divided into C-terminal inactivation, N-terminal inactivation and other non-inactivation referring the standard of Mondaca et al [30] and those of *TP53* referring Hung-Chih Hsu [31].

Statistical analysis

All statistical analyses were conducted in the R-project (version 4.2.1). The mutation landscape heat maps and the pathological pathways in PD-L1 positive cohorts were depicted by R package "maftools" [32]. R package "ggplot2" [33] and "corrplot" [34] were used to drawn the box plots and triangle heat maps of mutation frequency difference of important gene sites in PD-L1 positive/negative cohorts, respectively. The "fisher.test" function in R was implemented to calculate the significance of proportion difference between groups.

Results

Demographic characteristics of included patients

From 2021 to 2023, 752 patients pathologically diagnosed with colorectal cancer or intestinal cancer were enrolled in the present study. As shown in **Table 1**, the age and TMB status of the entire enrolled cohort are unrelated to PD-L1 positivity. However, after stratifying by PD-L1 expression level, female patients were more enriched in the PD-L1 positive group. At the same time, MSI-H status was positively related to PD-L1 positivity, suggesting that PD-L1 status may also be a noteworthy indicator similar to MSI. In addition, no statistic shifts are observed in cohort TMB or MSI grouped by age or gender (Table S1), except for the

acknowledged positive correlation between MSI and age, which indicates that there is no clear cohort preference for any type of gender or age in terms of MSI or TMB. More detailed characteristics of the cohort are demonstrated in **Table 1**.

Mutation profiling

The overall genotype landscape, stratified by PD-L1 status, is hierarchically colored depending on the number of mutations in corresponding genes, as shown in **Figure 1A** and **1B**. The top 10 most mutated genes are basically consistent (8/10) in both the PD-L1 positive group and PD-L1 negative group, including *TP53*, *KRAS*, *APC*, *PIK3CA*, *LRP1B*, *KMT2C*, *FAT1*, *FBXW7* (61% vs. 71%, 60% vs. 46%, 49% vs. 66%, 25% vs. 18%, 18% vs. 16%, 17% vs. 21, 14% vs. 13% and 11% vs. 12%; positive vs. negative, respectively). As depicted in **Figure 1C** and **1D**, the co-occurrence of mutations is more common in the PD-L1 negative group. The mutual exclusion between *BRAF* and *KRAS* or *APC* is not affected by the PD-L1 grouping, while the mutual exclusion between *KRAS* and *TP53* is weakened in the PD-L1 positive group.

Distinct pathogenic pathways in PD-L1 positive/negative groups

Some studies have mentioned that pathway-induced oncogenic constructive PD-L1 upregulation, rather than a lack of pre-existing immune responses, may be the reason for a patient's primary resistance to ICIs [26]. Thus, an analysis for the frequency of oncogenic pathway alterations between PD-L1-positive status and PD-L1-negative statuses was conducted, indicating a positive correlation between the RTK/RAS (*KRAS* and *BRAF*) signaling pathway and PD-L1 positive expression with statistical significance ($P < 0.001$, **Figure 2A**). Additionally, the Wnt and p53 signal pathways were found to be negatively related to PD-L1 expression, showing statistically significant differences ($P < 0.001$ and $P < 0.01$, **Figure 2A**).

We further performed a comparative analysis of mutations between PD-L1-positive and PD-L1-negative statuses, revealing a significant difference in the mutation frequency of four oncogenic genes (*APC*, *TP53*, *BRAF* and *KFAS*; **Figure 2B**, $P < 0.05$), which accounted for the

corresponding differences in signaling pathways aforementioned. A detailed display of the frequency of concurrent oncogenic alterations in these four important oncogenic genes is demonstrated in **Figure 2C**.

Subtypic view of important genes mutation frequency by PD-L1 expression hierarchy

Gene molecular typing can more clearly demonstrate the differences in oncogenic pathways caused by PD-L1 status stratification. Therefore, we analyzed the distribution percentage of PD-L1 status among important gene subtypes (**Figure 3A**) and demonstrated the distribution of mutations and their positions in Figure S1. *BRAF-V600E* ($P < 0.001$, compared to wild type), *KRAS-G12*, and *KRAS-G13* ($P < 0.05$ and $P < 0.01$, compared to wild type) mutation frequencies both display a distinct positive correlation to PD-L1 positivity, as shown in **Table 2**; **Figure 3A** and **3B**. Along with more detailed insight into *KRAS* mutations sites, G13D accounts for the clearly higher G13 mutation frequency in PD-L1 positive group compared to that in the negative group (data not shown).

Due to a considerable kinds of mutation sites, unlike oncogenes, which are simply divided into subtypes based on mutation sites, tumor suppressor gene subgroups are divided by mutation regions referring to previous studies [30, 31]. *APC* mutations are categorized by the mutation coordinate into N-terminal inactivation (*APC-N*), C-terminal inactivation (*APC-C*), other non-inactivation mutations (*APC*-other), and wild type [30]. No significant mutation distribution difference is caused by PD-L1 stratification between *APC-C* and *APC-N*. However, a distinct difference is observed between *APC-C* and wild type ($P < 0.001$, **Figure 2**, with more *APC-C* in the PD-L1 negative cohort) as well as between *APC-N* and wild type ($P = 0.051$, fisher's exact test, with more *APC-N* in the PD-L1 negative cohort). Similarly, *TP53* mutations are classified into DNA binding domain and others according to the variance coordinates [31]. Compared with the wild type, an enrichment of *TP53* other mutations is observed in the PD-L1 negative cohort ($P < 0.05$). The above subtypes with higher or lower mutation frequency compared with wild types may indicate some new explanations on the pathway mechanisms related to oncogenesis and progression.
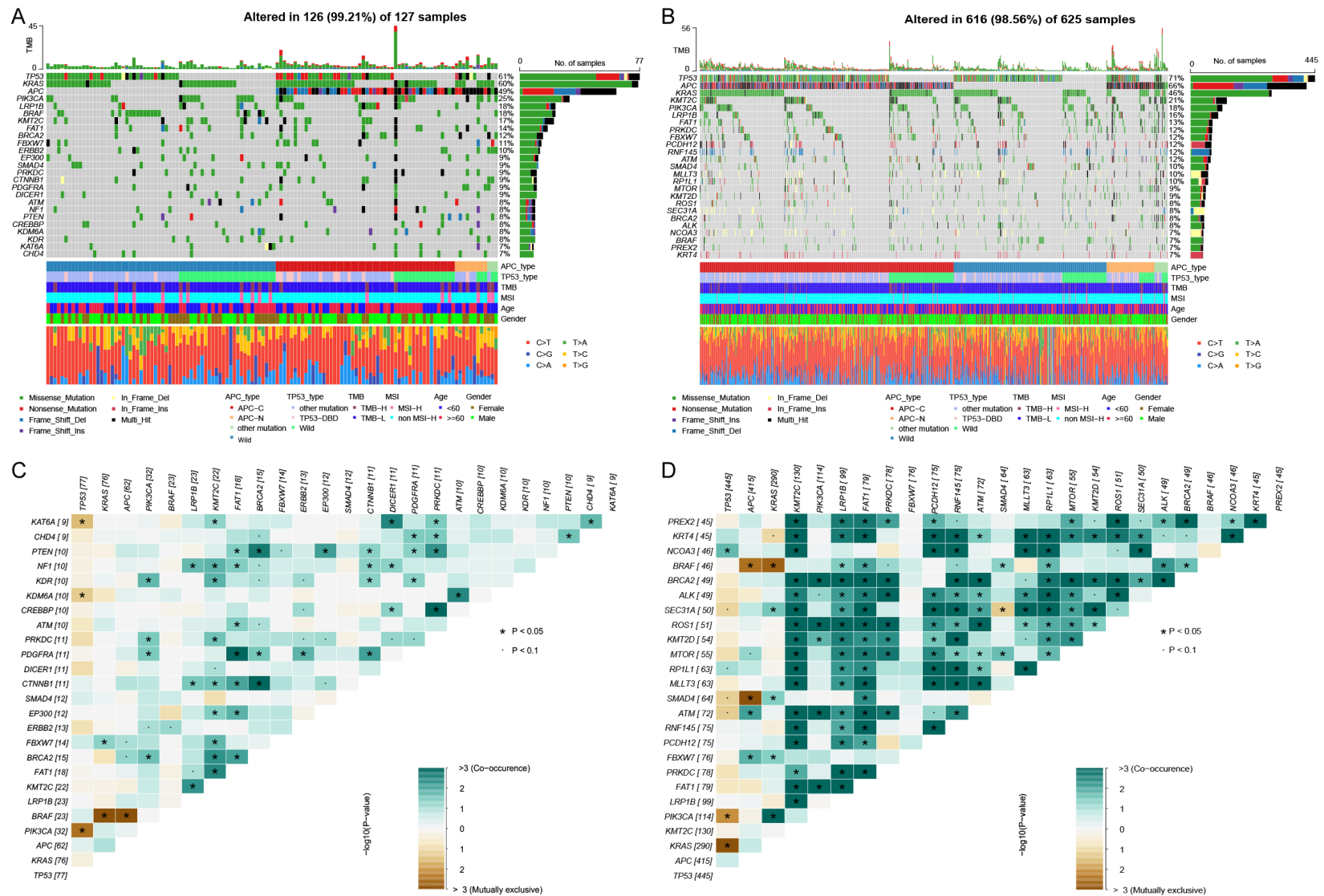
Figure 1. The water-fall diagram of the Top 25 mutated genes and their variant types in PD-L1 positive (A) and negative (B) advanced CRC tissues based on next generation sequencing data from collected samples. Co-occurrence and mutually exclusive relationships at gene-level are analyzed and plotted by R pack "maftools" for PD-L1 positive (C) and negative (D) cohort. Top 25 genes with the most distinct relationship are shown.
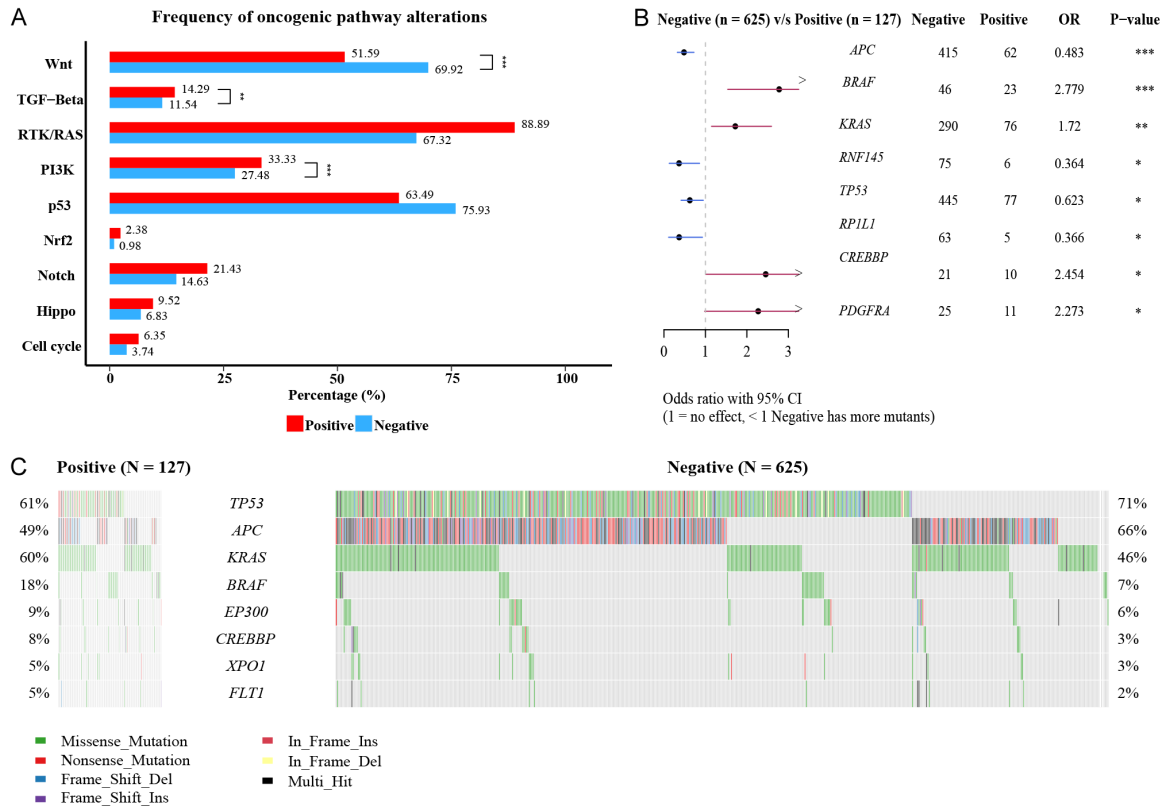
Figure 2. A. Frequency of oncogenic pathway alterations by PD-L1 status. B. Count of oncogenic pathway-related gene alterations by PD-L1 status. C. Frequency of concurrent oncogenic alterations by PD-L1 status. Note: * denotes P < 0.05; **, P < 0.01; ***, P < 0.001, Fisher's exact test.

Subtypic view of immunotherapy potential in PD-L1 positive cohort

Considering that TMB and MSI are both approved to be the biomarker of immunotherapy recently [9], we display the TMB and MSI distribution in the subtypes of important genes related to the pathological pathway in PD-L1 positive cohorts (Table S2; **Figure 4A** and **4B**). The distribution of TMB and MSI in the subgroup is basically consistent. PD-L1 positive patients with *TP53* and *KRAS* wild type, as well as patients carrying *APC-N*, *BRAF*-other and *KRAS*-other mutations may benefit from combining immunotherapy drugs with the original treatment schemes. Compared to its wild type, *KRAS*-other is the only subtype with a higher proportion of TMB-H status (P < 0.01, **Figure 4C** and **4D**). TMB-L and non MSI-H are significantly enriched in patients with *KRAS-G12* and *KRAS-G13* mutations, which may explain the poor curative effect of ICIs as a monotherapy for such patients. However, the population of PD-L1 positive patients is relatively small, with

only one or two patients carrying mutations in some subtypes (such as *APC-N*, *BRAF*-other), indicating that more data are required to draw a more accurate conclusion.

Subtypic view of immunotherapy potential in PD-L1 negative cohort

The distribution of TMB and MSI in the subgroup is also basically consistent in the PD-L1 negative group, with only the distribution in *KRAS-G13* mutations showing significant differences in the population stratified by PD-L1 status (Table S3; **Figure 5A** and **5B**). PD-L1 negative patients with wild type of *TP53* genes, and patients carrying *APC*-other, *BRAF*-other, *KRAS*-other and *KRAS*-G13 mutations, significantly represent TMB-H or MSI-H (**Figure 5C** and **5D**), suggesting potential benefit from combining immunotherapy drugs with the original treatment schemes. It is noteworthy that these results are consistent with previous studies on the relationship between TMB and *APC* subtyping [35] in the PD-L1 positive group, but are in
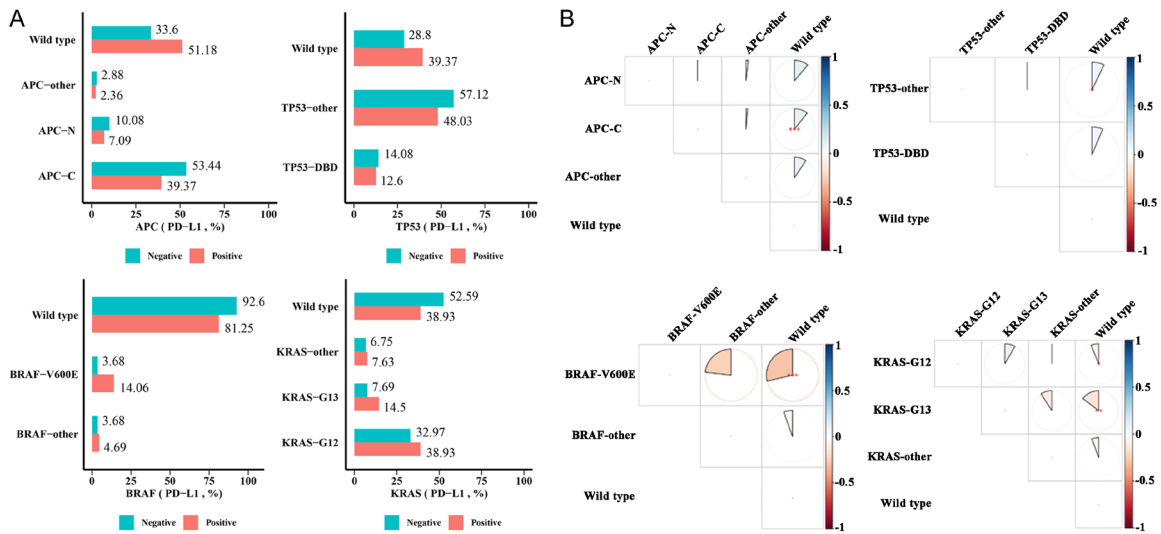
Figure 3. Comparison of PD-L1 status distribution percentage among important gene subtypes in total patient population (A). The difference of PD-L1 positivity rate in subtypes between pairwise groups are presented by fan plots (B). Red fan diagram denotes lower positivity rate in the corresponding column than that in row and blue one denotes the opposite. Fisher's exact test is applied in this analysis. Note: * denotes $P < 0.05$; **, $P < 0.01$; ***, $P < 0.001$.

Table 2. Site view of important genes mutation frequency in PD-L1 positive/negative groups

	PD-L1 positive No. (%) (n=127)	PD-L1 negative No. (%) (n=625)
[a]APC-N	9 (7.09)	63 (10.08)
[b]APC-C	50 (39.37)	334 (53.44)
[c]APC-other	3 (2.36)	18 (2.88)
Wild type	65 (51.18)	210 (33.60)
[d]TP53-other	61 (48.03)	357 (57.12)
[e]TP53-DBD	16 (12.60)	88 (14.08)
Wild type	50 (39.37)	180 (28.8)
BRAF-V600E	18 (14.17)	23 (3.68)
[f]BRAF-other	6 (4.72)	23 (3.68)
Wild type	104 (81.89)	579 (92.64)
KRAS-G12	51 (40.15)	210 (33.60)
KRAS-G13	19 (14.96)	49 (7.84)
[g]KRAS-other	10 (7.87)	43 (6.88)
Wild type	51 (40.16)	335 (53.6)

Note: [a]inactivation mutations on the N-terminal; [b]inactivation mutations on the C-terminal; [c]non-inactivation mutations; [d]mutations outside the protein-binding region; [e]mutations in the protein-binding region; [f]mutations other than V600E; [g]mutations other than G12X nor G13X.

contrast with them in PD-L1 negative groups, which may account for the lack of PD-L1 stratification previously. Coincidentally, these four subtypes (*APC*-other, *TP53* wild type, *BRAF*-other and *KRAS*-other) also showed significant-

ly higher levels of TMB or MSI in the PD-L1 positive patient group, suggesting that the immunotherapy potential of related subtypes may not be related to PD-L1 expression. At the same time, the proportion of *KRAS*-G13 subtypes showed significant differences between the PD-L1 positive and negative groups, suggesting that the tumor microenvironment of these two molecular subtypes and immunotherapy may require attention to the patient's PD-L1 status.

Discussion

PD-L1 is one of the widely studied biomarkers for solid tumor, and its expression level reflects the degree of immunosuppression in the tumor microenvironment to some extent. Even though PD-L1 cannot individually predict the efficacy of ICIs in CRC to date [24], more in-depth studies and detailed analyses are still required to elucidate its role in displaying the tumor microenvironment and cell-intrinsic immune programs, as well as the mechanisms behind the poor association between PD-L1 positivity and immunotherapy efficacy [36]. The PD-L1 positivity might result from immune response-induced PD-L1 expression or oncogenic constructive PD-L1 upregulation. The latter commonly demonstrates resistance to PD-1/PD-L1 therapies due to the lack of pre-existing immune response [26]. From the perspective of patho-
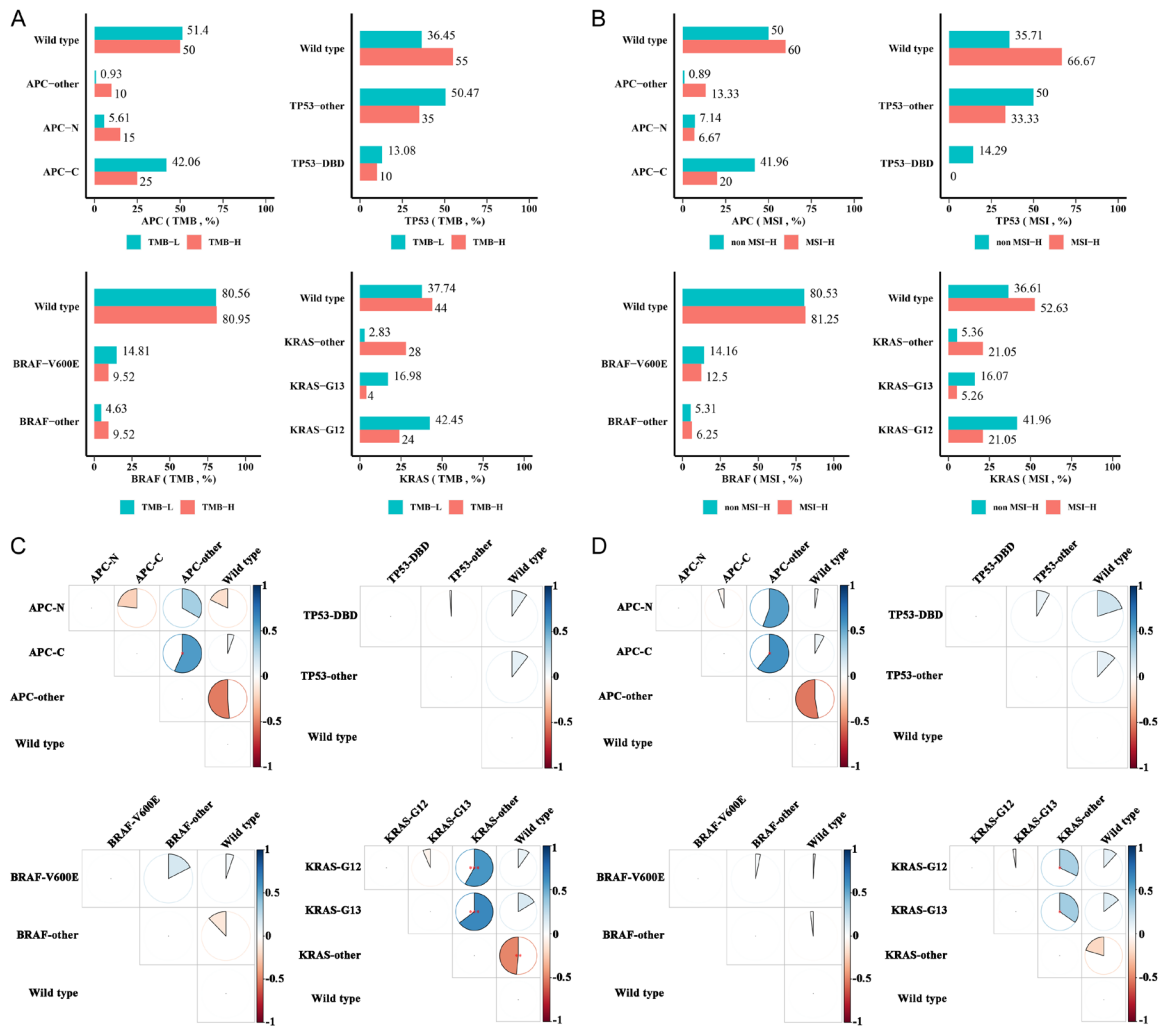
Figure 4. Percentage distribution of TMB status in PD-L1 positive patient cohort who carries important oncogenic gene mutations in advanced colon cancer (A) and distribution of MSI status (B). Subtype-level TMB positivity rate difference and corresponding statistical significance between gene subtypes are calculated pairwise in PD-L1 positive cohorts (C), where TMB positivity rate in each subtype is obtained by dividing the number of TMB-positive patients carrying the mutations of the subtype by the total patients of this subtype. Subtype-level MSI positivity rate difference and corresponding statistical significance (D). TMB and MSI expression are categorized into high level and low level by the aforementioned criterion and the distribution difference of TMB and MSI in each pairwise subtype is examined by Fisher's exact test. Red fan diagram denotes lower positivity rate in the corresponding column than that in row and blue one denotes the opposite. The size of the fan shaped coloring area corresponds to the value of positivity rate difference. Note: * denotes P < 0.05; **, P < 0.01; ***, P < 0.001.

logical pathways, we found that the RTK/RAS pathway (*KRAS* and *BRAF* mutations) is enriched in PD-L1 positive populations, while Wnt (*APC* mutations) and p53 (*TP53* mutations) are enriched in PD-L1 negative populations in our study. These findings are all related to oncogenic construction [37-40]. In previous research on the RTK/RAS pathways in CRC, *KRAS* mutations have been associated with down-regulation of immune pathways and a reduced number of tumor infiltrating lymphocytes (TILs) [41], which are considered markers for worse sur-

vival at all disease stages [42]. Additionally, a study of triple-negative breast cancer also found that alterations in RTK/RAS signaling were correlated with low TIL numbers, which in turn correlated with worse recurrence-free survival [42]. The association between PD-L1 positivity and the RTK/RAS pathway may be the reason for the poor prognosis in PD-L1 positive CRC cohort.

According to studies on therapeutic valuable targets in the treatment of CRC, it is almost
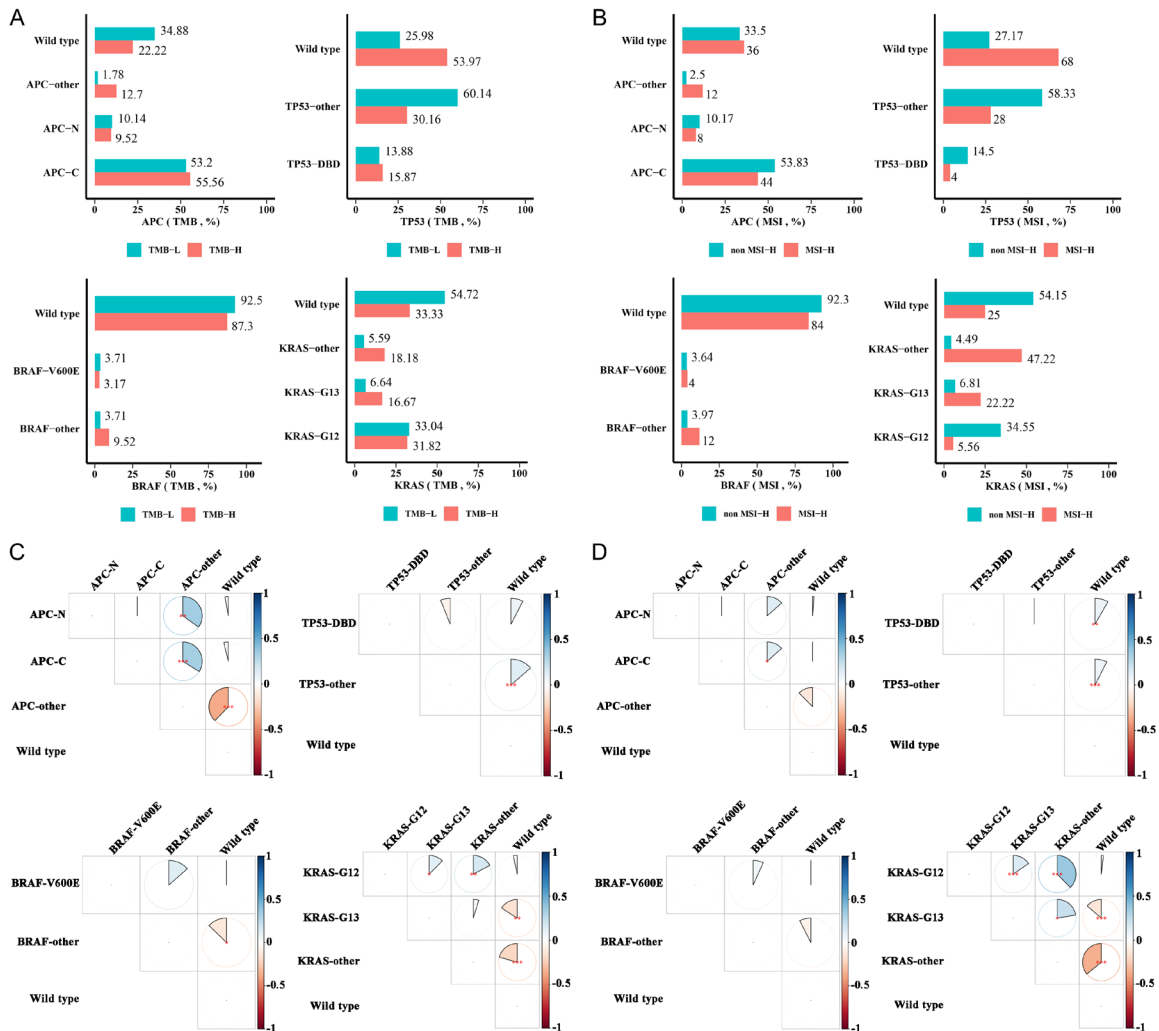
Figure 5. Percentage distribution of TMB status in PD-L1 negative patient cohort who carries important oncogenic gene mutations in advanced colon cancer (A) and distribution of MSI status (B). Subtype-level TMB positivity rate difference and corresponding statistical significance between gene subtypes are calculated pairwise in PD-L1 negative cohorts (C), where TMB positivity rate in each subtype is obtained by dividing the number of TMB-positive patients carrying the mutations of the subtype by the total patients of this subtype. Subtype-level MSI positivity rate difference and corresponding statistical significance (D). TMB and MSI expression are categorized into high level and low level by the aforementioned criterion and the distribution difference of TMB and MSI in each pairwise subtype is examined by Fisher's exact test. Red fan diagram denotes lower positivity rate in the corresponding column than that in row and blue one denotes the opposite. The size of the fan shaped coloring area corresponds to the value of positivity rate difference. Note: * denotes P < 0.05; **, P < 0.01; ***, P < 0.001.

impossible for p53 drugs to be used as monotherapy for cancer treatment [43]. As for the Wnt/β-catenin signaling pathway, several inhibitors have been developed for CRC treatment. However, so far no molecular therapeutics targeting this pathway have been incorporated into oncological practice [37]. A recent noteworthy proof-of-concept clinical trial [44], which combines ICIs with genomic stratification of the RTK/RAS pathway to improve effectiveness in clinically troublesome non-MSI-H subtypes,

indicates an intriguing approach: considering the tumor microenvironment indicated by PD-L1 status and the genomic characteristics of the cohort may improve the clinical effect in some combined therapy strategies.

Currently, there are few personalized treatment schemes for PD-L1 negative patients, who account for the majority of total patient population. Considering the extremely effectiveness of ICIs for mCRC patients with MSI-H status [45],

screening out genomic subtypes which are enriched in MSI-H or TMB-H status may improve the immunotherapy efficacy of ICIs for the corresponding subtype population. In this study, we found that PD-L1 negative patients with wild type of *APC* and *KRAS* genes, as well as those carrying *APC-C*, *TP53*-other, and *KRAS-G12* mutations demonstrated significantly higher MSI-H or non-conflictingly corresponding TMB-H levels. This indicates a potential for these patient populations to gain more benefits from ICIs treatments. A recent single-arm phase II clinical trial, LCCC1632 (NCT03442569), targeting *KRAS/NRAS/BRAF* wild-type MSS refractory mCRC demonstrated a promising breakthrough in the combination of ICIs and anti-angiogenic drugs [46, 47]. Considering that targeting *KRAS* has become less difficult recently and one of the FDA-approved *KRAS* inhibitors, Sotorasib, has shown anticancer activity in patients with *KRAS G12C*-mutated advanced solid tumors [48-50]. In our study, CRC patients with *KARS-G12* exhibited similar low MSI and TMB status to that of wild type, may also benefit from the scheme similar to LCCC1632, which combines take combined-therapy including ICIs for subtypes with MSS status.

Notably, there are several limitations to this study. Firstly, it is a single-center retrospective study without treatment follow-up data. More promising multicenter studies with larger cohorts and long-term follow-up data are needed for a better understanding of the relationship between these gene mutations and ICIs therapy efficacy. Secondly, the tumor tissues used in this study can only depict a limited range of solid tumors in a single time-frame, which is inadequate to characterize the full view because of intra-tumoral and inter-metastatic heterogeneity.

In conclusion, our study developed a potentially valuable approach to stratifying advanced colorectal patient based on PD-L1 expression levels and pathway-related molecular subtypes. We identified one pathological pathway (RTK/RAS) positively related to PD-L1 expression levels and two pathways (Wnt and p53) negatively related to PD-L1 expression. We investigated the detailed distribution preference of PD-L1 in corresponding gene subtypes. Furthermore, we found that patients with *APC*-other, *TP53* wild type, *BRAF*-other and *KRAS*-other mutations showed a significantly higher proportion of TMB-H or MSI-H, regardless of PD-L1 status. This suggests that the immunotherapy potential of these subtypes may not be related to PD-L1 expression. Additionally, the high of TMB or MSI in *KRAS-G13* subtypes showed significant differences between PD-L1 positive and negative groups, indicating that PD-L1 stated may require attention for patients with these molecular subtypes when considering ICIs treatments. Our study may provide potential implications on the strategy of combining immune checkpoint inhibitors and pathway-targeted therapy.

Disclosure of conflict of interest

Wei Wen, Xiaokai Zhao, Jieyi Li, Pengmin Yang, Daoyun Zhang, and Ziying Gong were employed by the Jiaxing Yunying Medical Inspection Co., Ltd., and the Zhejiang Yunying Medical Technology Co., Ltd. The remaining authors declare that the research was conducted in the absence of any commercial or financial relationships that could be construed as a potential conflict of interest.

Address correspondence to: Mingliang Wang, Department of General Surgery, RuiJin Hospital Lu Wan Branch, Shanghai Jiaotong University School of Medicine, No. 197 Ruijin Second Road, Huangpu District, Shanghai 200020, China. Tel: +86-21-64458887; Fax: +86-21-64458887; E-mail: wml_2902@163.com; Ziying Gong, Jiaxing Key Laboratory of Precision Medicine and Companion Diagnostics, Jiaxing Yunying Medical Inspection Co., Ltd., No. 153 Huixin Road, Nanhu District, Jiaxing 314000, Zhejiang, China. Tel: +86-573-83108883; E-mail: gzy@yunyingmedicine.com; Daoyun Zhang, Depart-

ment of R&D, Zhejiang Yunying Medical Technology Co., Ltd., Building 5, No. 3556 Linggongtang Road, Nanhu District, Jiaxing 314000, Zhejiang, China. Tel: +86-573-83108883; E-mail: zdy@yunyingmedicine. com

References

[1] Cristescu R, Mogg R, Ayers M, Albright A, Murphy E, Yearley J, Sher X, Liu XQ, Lu H, Nebozhyn M, Zhang C, Lunceford JK, Joe A, Cheng J, Webber AL, Ibrahim N, Plimack ER, Ott PA, Seiwert TY, Ribas A, McClanahan TK, Tomassini JE, Loboda A and Kaufman D. Pan-tumor genomic biomarkers for PD-1 checkpoint blockade-based immunotherapy. Science 2018; 362: eaar3593.

[2] Andre T, Shiu KK, Kim TW, Jensen BV, Jensen LH, Punt CJA, Smith DM, Garcia-Carbonero R, Benavides M, Gibbs P, De La Fouchardiere C, Rivera F, Elez E, Bendell JC, Le DT, Yoshino T, Yang P, Farooqui MZH, Marinello P and Diaz LA. Pembrolizumab versus chemotherapy for microsatellite instability-high/mismatch repair deficient metastatic colorectal cancer: the phase 3 KEYNOTE-177 Study. J Clin Oncol 2020; 38: LBA4.

[3] Le DT, Uram JN, Wang H, Bartlett B, Kemberling H, Eyring A, Azad NS, Laheru D, Donehower RC, Crocenzi TS, Goldberg RM, Fisher GA, Lee JJ, Greten TF, Koshiji M, Kang SP, Anders RA, Eshleman JR, Vogelstein B and Diaz LA. Programmed death-1 blockade in mismatch repair deficient colorectal cancer. J Clin Oncol 2016; 34: 103.

[4] Chen EX, Jonker DJ, Loree JM, Kennecke HF, Berry SR, Couture F, Ahmad CE, Goffin JR, Kavan P, Harb M, Colwell B, Samimi S, Samson B, Abbas T, Aucoin N, Aubin F, Koski SL, Wei AC, Magoski NM, Tu D and O'Callaghan CJ. Effect of combined immune checkpoint inhibition vs best supportive care alone in patients with advanced colorectal cancer: the Canadian Cancer Trials Group CO.26 Study. JAMA Oncol 2020; 6: 831-838.

[5] Parikh AR, Clark JW, Wo JYL, Yeap BY, Allen JN, Blaszkowsky LS, Ryan DP, Giantonio BJ, Weekes CD, Zhu AX, Van Seventer EE, Matlack L, Foreman B, Ly L, Drapek LC, Ting DT, Corcoran RB and Hong TS. A phase II study of ipilimumab and nivolumab with radiation in microsatellite stable (MSS) metastatic colorectal adenocarcinoma (mCRC). J Clin Oncol 2019; 37: 3514.

[6] Bendell JC, Kim TW, Goh BC, Wallin J, Oh DY, Han SW, Lee CB, Hellmann MD, Desai J, Lewin JH, Solomon BJ, Chow LQM, Miller WH, Gainor JF, Flaherty K, Infante JR, Das-Thakur M, Foster P, Cha E and Bang YJ. Clinical activity and safety of cobimetinib (cobi) and atezolizumab in colorectal cancer (CRC). J Clin Oncol 2016; 34: 3502.

[7] Bendell JC, Bang YJ, Chee CE, Ryan DP, McRee AJ, Chow LQ, Desai J, Wongchenko M, Yan Y, Pitcher B, Foster P, Cha E, Grossman W and Kim TW. A phase Ib study of safety and clinical activity of atezolizumab (A) and cobimetinib (C) in patients (pts) with metastatic colorectal cancer (mCRC). J Clin Oncol 2018; 36: 560.

[8] Hochster HS, Bendell JC, Cleary JM, Foster P, Zhang W, He X, Hernandez G, Iizuka K and Eckhardt SG. Efficacy and safety of atezolizumab (atezo) and bevacizumab (bev) in a phase Ib study of microsatellite instability (MSI)-high metastatic colorectal cancer (mCRC). J Clin Oncol 2017; 35: 673.

[9] Fan A, Wang B, Wang X, Nie Y, Fan D, Zhao X and Lu Y. Immunotherapy in colorectal cancer: current achievements and future perspective. Int J Biol Sci 2021; 17: 3837-3849.

[10] Yarchoan M, Hopkins A and Jaffee EM. Tumor mutational burden and response rate to PD-1 inhibition. N Engl J Med 2017; 377: 2500-2501.

[11] Panda A, Betigeri A, Subramanian K, Ross JS, Pavlick DC, Ali S, Markowski P, Silk A, Kaufman HL, Lattime E, Mehnert JM, Sullivan R, Lovly CM, Sosman J, Johnson DB, Bhanot G and Ganesan S. Identifying a clinically applicable mutational burden threshold as a potential biomarker of response to immune checkpoint therapy in solid tumors. JCO Precis Oncol 2017; 2017: PO.17.00146.

[12] Lau D, Kalaitzaki E, Church DN, Pandha H, Tomlinson I, Annels N, Gerlinger M, Sclafani F, Smith G, Begum R, Crux R, Gillbanks A, Wordsworth S, Chau I, Starling N, Cunningham D and Dhillon T. Rationale and design of the POLEM trial: avelumab plus fluoropyrimidine-based chemotherapy as adjuvant treatment for stage III mismatch repair deficient or POLE exonuclease domain mutant colon cancer: a phase III randomised study. ESMO Open 2020; 5: e000638.

[13] Hu H, Cai W, Wu D, Hu W, Dong Wang L, Mao J, Zheng S and Ge W. Ultra-mutated colorectal cancer patients with POLE driver mutations exhibit distinct clinical patterns. Cancer Med 2021; 10: 135-142.

[14] Flecchia C, Zaanan A, Lahlou W, Basile D, Broudin C, Gallois C, Pilla L, Karoui M, Manceau G and Taieb J. MSI colorectal cancer, all you need to know. Clin Res Hepatol Gastroenterol 2022; 46: 101983.

[15] Harada S and Morlote D. Molecular pathology of colorectal cancer. Adv Anat Pathol 2020; 27: 20-26.

[16] Martelli V, Pastorino A and Sobrero AF. Prognostic and predictive molecular biomarkers in advanced colorectal cancer. Pharmacol Ther 2022; 236: 108239.

[17] Chalmers ZR, Connelly CF, Fabrizio D, Gay L, Ali SM, Ennis R, Schrock A, Campbell B, Shlien A, Chmielecki J, Huang F, He Y, Sun J, Tabori U, Kennedy M, Lieber DS, Roels S, White J, Otto GA, Ross JS, Garraway L, Miller VA, Stephens PJ and Frampton GM. Analysis of 100,000 human cancer genomes reveals the landscape of tumor mutational burden. Genome Med 2017; 9: 34.

[18] Chabanon RM, Pedrero M, Lefebvre C, Marabelle A, Soria JC and Postel-Vinay S. Mutational landscape and sensitivity to immune checkpoint blockers. Clin Cancer Res 2016; 22: 4309-4321.

[19] Yarchoan M, Albacker LA, Hopkins AC, Montesion M, Murugesan K, Vithayathil TT, Zaidi N, Azad NS, Laheru DA, Frampton GM and Jaffee EM. PD-L1 expression and tumor mutational burden are independent biomarkers in most cancers. JCI Insight 2019; 4: e126908

[20] Yang L, Xue R and Pan C. Prognostic and clinicopathological value of PD-L1 in colorectal cancer: a systematic review and meta-analysis. Onco Targets Ther 2019; 12: 3671-3682.

[21] Wang S, Yuan B, Wang Y, Li M, Liu X, Cao J, Li C and Hu J. Clinicopathological and prognostic significance of PD-L1 expression in colorectal cancer: a meta-analysis. Int J Colorectal Dis 2021; 36: 117-130.

[22] Alexander PG, McMillan DC and Park JH. A meta-analysis of CD274 (PD-L1) assessment and prognosis in colorectal cancer and its role in predicting response to anti-PD-1 therapy. Crit Rev Oncol Hematol 2021; 157: 103147.

[23] Le DT, Uram JN, Wang H, Bartlett BR, Kemberling H, Eyring AD, Skora AD, Luber BS, Azad NS, Laheru D, Biedrzycki B, Donehower RC, Zaheer A, Fisher GA, Crocenzi TS, Lee JJ, Duffy SM, Goldberg RM, de la Chapelle A, Koshiji M, Bhaijee F, Huebner T, Hruban RH, Wood LD, Cuka N, Pardoll DM, Papadopoulos N, Kinzler KW, Zhou S, Cornish TC, Taube JM, Anders RA, Eshleman JR, Vogelstein B and Diaz LA Jr. PD-1 blockade in tumors with mismatch-repair deficiency. N Engl J Med 2015; 372: 2509-2520.

[24] Overman MJ, Lonardi S, Leone F, McDermott RS, Morse MA, Wong KYM, Neyns B, Leach JL, Garcia Alfonso P, Lee JJ, Hill A, Lenz HJ, Desai J, Moss RA, Cao ZA, Ledeine JM, Tang H, Kopetz S and Andre T. Nivolumab in patients with DNA mismatch repair deficient/microsatellite instability high metastatic colorectal cancer: update from CheckMate 142. J Clin Oncol 2017; 35: 519.

[25] Peng QH, Wang CH, Chen HM, Zhang RX, Pan ZZ, Lu ZH, Wang GY, Yue X, Huang W and Liu RY. CMTM6 and PD-L1 coexpression is associated with an active immune microenvironment and a favorable prognosis in colorectal cancer. J Immunother Cancer 2021; 9: e001638.

[26] Yi M, Niu M, Xu L, Luo S and Wu K. Regulation of PD-L1 expression in the tumor microenvironment. J Hematol Oncol 2021; 14: 10.

[27] Zhao T, Li Y, Zhang J and Zhang B. PD-L1 expression increased by IFN-gamma via JAK2-STAT1 signaling and predicts a poor survival in colorectal cancer. Oncol Lett 2020; 20: 1127-1134.

[28] Shen Z, Gu L, Mao D, Chen M and Jin R. Clinicopathological and prognostic significance of PD-L1 expression in colorectal cancer: a systematic review and meta-analysis. World J Surg Oncol 2019; 17: 4.

[29] Han X, Zhang S, Zhou DC, Wang D, He X, Yuan D, Li R, He J, Duan X, Wendl MC, Ding L and Niu B. MSIsensor-ct: microsatellite instability detection using cfDNA sequencing data. Brief Bioinform 2021; 22: bbaa402.

[30] Mondaca S, Walch H, Nandakumar S, Chatila WK, Schultz N and Yaeger R. Specific Mutations in APC, but not alterations in DNA damage response, associate with outcomes of patients with metastatic colorectal cancer. Gastroenterology 2020; 159: 1975-1978, e1974.

[31] Hsu HC, You JF, Chen SJ, Chen HC, Yeh CY, Tsai WS, Hung HY, Yang TS, Lapke N and Tan KT. TP53 DNA binding domain mutations predict progression-free survival of bevacizumab therapy in metastatic colorectal cancer. Cancers (Basel) 2019; 11: 1079.

[32] Mayakonda A, Lin DC, Assenov Y, Plass C and Koeffler HP. Maftools: efficient and comprehensive analysis of somatic variants in cancer. Genome Res 2018; 28: 1747-1756.

[33] Wickham H. ggplot2: Elegant Graphics for Data Analysis. New York: Springer-Verlag; 2016.

[34] Simko V and Wei T. R package 'corrplot': visualization of a Correlation Matrix (Version 0.92). 2021.

[35] Peng H, Ying J, Zang J, Lu H, Zhao X, Yang P, Wang X, Li J, Gong Z, Zhang D and Wang Z. Specific mutations in APC, with prognostic implications in metastatic colorectal cancer. Cancer Res Treat 2023; 55: 1270-1280.

[36] Shen X and Zhao B. Efficacy of PD-1 or PD-L1 inhibitors and PD-L1 expression status in cancer: meta-analysis. BMJ 2018; 362: k3529.

[37] Cheng X, Xu X, Chen D, Zhao F and Wang W. Therapeutic potential of targeting the Wnt/beta-catenin signaling pathway in colorectal can-

cer. Biomed Pharmacother 2019; 110: 473-481.

[38] Zheng CC, Liao L, Liu YP, Yang YM, He Y, Zhang GG, Li SJ, Liu T, Xu WW and Li B. Blockade of nuclear beta-catenin signaling via direct targeting of RanBP3 with NU2058 induces cell senescence to suppress colorectal tumorigenesis. Adv Sci (Weinh) 2022; 9: e2202528.

[39] Liao H, Li X, Zhao L, Wang Y, Wang X, Wu Y, Zhou X, Fu W, Liu L, Hu HG and Chen YG. A PROTAC peptide induces durable beta-catenin degradation and suppresses Wnt-dependent intestinal cancer. Cell Discov 2020; 6: 35.

[40] Zhang W, Sun R, Zhang Y, Hu R, Li Q, Wu W, Cao X, Zhou J, Pei J and Yuan P. Cabazitaxel suppresses colorectal cancer cell growth via enhancing the p53 antitumor pathway. FEBS Open Bio 2021; 11: 3032-3050.

[41] Lal N, White BS, Goussous G, Pickles O, Mason MJ, Beggs AD, Taniere P, Willcox BE, Guinney J and Middleton GW. KRAS mutation and consensus molecular subtypes 2 and 3 are independently associated with reduced immune infiltration and reactivity in colorectal cancer. Clin Cancer Res 2018; 24: 224-233.

[42] Sillo TO, Beggs AD, Morton DG and Middleton G. Mechanisms of immunogenicity in colorectal cancer. Br J Surg 2019; 106: 1283-1297.

[43] Hassin O and Oren M. Drugging p53 in cancer: one protein, many targets. Nat Rev Drug Discov 2023; 22: 127-144.

[44] Tian J, Chen JH, Chao SX, Pelka K, Giannakis M, Hess J, Burke K, Jorgji V, Sindurakar P, Braverman J, Mehta A, Oka T, Huang M, Lieb D, Spurrell M, Allen JN, Abrams TA, Clark JW, Enzinger AC, Enzinger PC, Klempner SJ, McCleary NJ, Meyerhardt JA, Ryan DP, Yurgelun MB, Kanter K, Van Seventer EE, Baiev I, Chi G, Jarnagin J, Bradford WB, Wong E, Michel AG, Fetter IJ, Siravegna G, Gemma AJ, Sharpe A, Demehri S, Leary R, Campbell CD, Yilmaz O, Getz GA, Parikh AR, Hacohen N and Corcoran RB. Combined PD-1, BRAF and MEK inhibition in BRAF(V600E) colorectal cancer: a phase 2 trial. Nat Med 2023; 29: 458-466.

[45] Lenz HJ, Overman MJ, Van Cutsem E, Limon ML, Wong MK, Hendlisz A, Aglietta M, Garcia-Alfonso P, Neyns B, Gelsomino F, Cardin DB, Dragovich T, Shah U, McCraith SM, Wang A, Lei M, Yao J, Jin L and Lonardi S. First-line (1L) nivolumab (NIVO) + ipilimumab (IPI) in patients (pts) with microsatellite instability-high/mismatch repair deficient (MSI-H/dMMR) metastatic colorectal cancer (mCRC): 64-month (mo) follow-up from CheckMate 142. J Clin Oncol 2023; 41: 3550.

[46] Lee MS, Loehrer PJ, Imanirad I, Cohen S, Ciombor KK, Moore DT, Carlson CA, Sanoff HK and McRee AJ. Phase II study of ipilimumab, nivolumab, and panitumumab in patients with KRAS/NRAS/BRAF wild-type (WT) microsatellite stable (MSS) metastatic colorectal cancer (mCRC). J Clin Oncol 2021; 39: 7.

[47] NIH-ClinicalTrials.gov. PhII Trial Panitumumab, Nivolumab, Ipilimumab in Kras/Nras/BRAF Wild-type MSS Refractory mCRC. 2020. https://classic.clinicaltrials.gov/ct2/show/NCT03442569.

[48] Skoulidis F, Li BT, Dy GK, Price TJ, Falchook GS, Wolf J, Italiano A, Schuler M, Borghaei H, Barlesi F, Kato T, Curioni-Fontecedro A, Sacher A, Spira A, Ramalingam SS, Takahashi T, Besse B, Anderson A, Ang A, Tran Q, Mather O, Henary H, Ngarmchamnanrith G, Friberg G, Velcheti V and Govindan R. Sotorasib for lung cancers with KRAS p.G12C mutation. N Engl J Med 2021; 384: 2371-2381.

[49] Blair HA. Sotorasib: first approval. Drugs 2021; 81: 1573-1579.

[50] Fakih MG, Kopetz S, Kuboki Y, Kim TW, Munster PN, Krauss JC, Falchook GS, Han SW, Heinemann V, Muro K, Strickler JH, Hong DS, Denlinger CS, Girotto G, Lee MA, Henary H, Tran Q, Park JK, Ngarmchamnanrith G, Prenen H and Price TJ. Sotorasib for previously treated colorectal cancers with KRAS(G12C) mutation (CodeBreaK100): a prespecified analysis of a single-arm, phase 2 trial. Lancet Oncol 2022; 23: 115-124.

Table S1. Cohort distribution information stratified by MSI status or TMB status

Tumor	Type		Age		[a]P	Gender		[a]P
			< 60	≥ 60		Male	Female	
Colorectal cancer	MSI	MSI-High	26	14	0.01*	22	18	0.3
		non MSI-H	312	400		456	256	
	TMB	TMB-High	45	38	0.09	50	33	0.6
		TMB-Low	293	376		428	241	

[a]P value are tested by Chi-square Test. * denotes P < 0.05.

Table S2. Subtypic view of MSI and TMB of important genes in PD-L1 positive group

	TMB-H No. (%)		TMB-L No. (%)		MSI-H No. (%)		non MSI-H No. (%)	
Total	20	15.75	107	84.25	15	11.81	112	88.19
APC-N	3	33.33	6	66.67	1	11.11	8	88.89
APC-C	5	10.00	45	90.00	3	6.00	47	94.00
APC-other	2	66.67	1	33.33	2	66.67	1	33.33
Wild type	10	15.38	55	84.62	9	13.85	56	86.15
Total	20	15.75	107	84.25	31	24.41	96	75.59
TP53-DBD	2	12.50	14	87.50	16	100.00	0	0.00
TP53-other	7	11.48	54	88.52	5	8.20	56	91.8
Wild type	11	22.00	39	78.00	10	20.00	40	80.00
Total	21	16.28	108	83.72	16	12.40	113	87.60
[a]BRAF V600E	2	11.11	16	88.89	2	11.11	16	88.89
[a]BRAF-other	2	28.57	5	71.43	1	14.29	6	85.71
Wild type	17	16.35	87	83.65	13	12.5	91	87.50
Total	25	19.08	106	80.92	19	14.50	112	85.50
[a]KRAS-G12	6	11.76	45	88.24	4	7.84	47	92.16
[a]KRAS-G13	1	5.26	18	94.74	1	5.26	18	94.74
[a]KRAS-other	7	70.00	3	30.00	4	40.00	6	60.00
Wild type	11	21.57	40	78.43	10	19.61	41	80.39

[a]The mutations of KRAS and BRAF are analyzed by site instead of by patient, which means 2 different mutated sites in one patient were categorized into their respective groups.

Table S3. Subtypic view of MSI and TMB of important genes in PD-L1 negative group (n = 625)

	TMB-H No. (%)		TMB-L No. (%)		MSI-H No. (%)		non MSI-H No. (%)	
Total	63	10.08	562	89.92	25	4.00	600	96.00
APC-N	6	9.50	57	90.50	2	3.20	61	96.80
APC-C	35	10.50	299	89.50	11	3.30	323	96.70
APC-other	8	44.40	10	55.60	3	16.70	15	83.30
Wild type	14	6.70	196	93.30	9	4.30	201	95.70
Total	63	10.08	562	89.92	25	4.00	600	96.00
TP53-DBD	10	11.40	78	88.60	1	1.10	87	98.90
TP53-other	19	5.30	338	94.70	7	2.00	350	98.00
Wild type	34	18.90	146	81.10	17	9.40	163	90.60
Total	63	10.02	566	89.98	25	3.97	604	96.03
[a]BRAF V600E	2	8.70	21	91.30	1	4.30	22	95.70
[a]BRAF-other	6	22.20	21	77.80	3	11.10	24	88.90
Wild type	55	9.50	524	90.50	21	3.60	558	96.40
Total	66	10.34	572	89.66	36	5.64	602	94.36
[a]KRAS-G12	21	10.00	189	90.00	2	1.00	208	99.00
[a]KRAS-G13	11	22.40	38	77.60	8	16.30	41	83.70
[a]KRAS-other	12	27.27	32	72.73	17	38.64	27	61.36
Wild type	22	6.60	313	78.90	9	2.7	326	97.3

[a]The mutations of KRAS and BRAF are analyzed by site instead of by patient, which means 2 different mutated sites in one patient were categorized into their respective groups.

Table S4. 639 targeted NGS panel list

| Gene name														
ABCA6	ABCB1	ABCC11	ABCC2	ABCC4	ABCF1	ABCG2	ABL1	ABL2	ACTR3B	ACVR1B	ADAMTS10	ADNP	AGAP9	AHNAK
AKAP7	AKR1C2	AKT1	AKT2	AKT3	ALK	AMER1	ANK2	ANKRD36	ANO10	APC	AR	ARAF	ARFRP1	ARHGAP5
ARID1A	ARID1B	ARID2	ART5	ASPM	ASXL1	ATM	ATR	ATRX	AURKA	AURKB	AXIN1	AXL	BAP1	BARD1
BAX	BCL2	BCL2L1	BCL2L11	BCL2L2	BCL6	BCL6B	BCOR	BCORL1	BCR	BEND5	BLM	BMPR2	BRAF	BRCA1
BRCA2	BRD3	BRD4	BRIP1	BTG1	BTK	C11orf30	C1orf144	C21orf58	C22orf31	C8orf34	CARD11	CASP5	CBFB	CBL
CBR3	CBWD6	CCDC144NL	CCKBR	CCND1	CCND2	CCND3	CCNE1	CCR5	CD274	CD3G	CD79A	CD79B	CDA	CDC27
CDC42EP1	CDC7	CDC73	CDCP2	CDH1	CDH5	CDK12	CDK4	CDK6	CDK8	CDKN1A	CDKN1B	CDKN2A	CDKN2B	CDKN2C
CEBPA	CENPH	CEP162	CEP164	CHD2	CHD4	CHEK1	CHEK2	CIC	CLASP1	CLDN16	CLIP1	CLOCK	CNDP1	COBLL1
COL5A3	CREBBP	CRKL	CRLF2	CROCC	CSF1R	CSMD3	CTCF	CTNNA1	CTNNB1	CUL3	CUZD1	CYB5R4	CYLD	CYP19A1
CYP1B1	CYP21A2	CYP2C19	CYP2C8	CYP2D6	CYP3A4	CYP3A5	CYP4B1	DAXX	DCP1B	DDHD1	DDR2	DDX11	DDX23	DEFB126
DHFR	DHX8	DICER1	DIEXF	DLEC1	DNMT3A	DOT1L	DPYD	DYNC2H1	EBPL	EGFR	EHBP1	ELFN1	EP300	EPCAM
EPHA3	EPHA5	EPHA7	EPHB1	ERBB2	ERBB3	ERBB4	ERCC1	ERCC2	ERG	ERRFI1	ESR1	ESR2	ESRRA	EZH2
F2RL2	FAM174B	FAM186A	FAM46C	FAM71E2	FANCA	FANCC	FANCD2	FANCE	FANCF	FANCG	FANCL	FAS	FAT1	FBXW7
FCAMR	FCGBP	FCGR3A	FCRLA	FGF10	FGF14	FGF19	FGF23	FGF3	FGF4	FGF6	FGFR1	FGFR2	FGFR3	FGFR4
FH	FKBP9	FLCN	FLT1	FLT3	FLT4	FMN2	FOPNL	FOXL2	FOXP1	FRS2	FUBP1	GABRA6	GATA1	GATA2
GATA3	GATA4	GATA6	GCNT2	GGH	GGT1	GID4	GLI1	GLTSCR1	GNA11	GNA13	GNAQ	GNAS	GNLY	GOLGA6L4
GOLGA6L6	GOT1L1	GPR124	GRIK2	GRIN2A	GRM3	GSK3B	GSTM5	GSTO1	GSTP1	H3F3A	HAVCR1	HGF	HIF1A	HIST1H3B
HLA	HMGXB4	HNF1A	HNRNPL	HRAS	HSD3B1	HSP90AA1	HSPA8	HTR1E	IDH1	IDH2	IFI27	IFITM3	IGF1R	IGF2
IKBKE	IKZF1	IL7R	INHBA	INPP4B	IRF2	IRF4	IRS2	ISX	ITPA	JAK1	JAK2	JAK3	JPH4	JUN
KANK3	KAT6A	KAT6B	KCNB2	KCNJ5	KDM5A	KDM5C	KDM6A	KDR	KEAP1	KEL	KIAA0355	KIAA1024	KIAA1211	KIF25
KIF6	KIT	KLF4	KLHL6	KMT2A	KMT2C	KMT2D	KPNA2	KRAS	KRT15	KRT4	KRTAP10	KRTAP4	KRTAP5	LCE1F
LCE4A	LGALS9B	LIG1	LIMCH1	LMAN1	LMO1	LOC105374608	LOC107986229	LOR	LRP1B	LRP2	LTA	LURAP1L	LYN	LZTR1
M6PR	MAGI2	MAN1B1	MAP2K1	MAP2K2	MAP2K4	MAP3K1	MCCC2	MCHR2	MCL1	MCMDC2	MDM2	MDM4	MED12	MED13
MEF2B	MEN1	MET	MITF	MLH1	MLLT3	MPL	MRE11A	MSH2	MSH3	MSH6	MTHFR	MTOR	MUC2	MUC4
MUC6	MUTYH	MVK	MYB	MYC	MYCL	MYCN	MYD88	MYL1	MYOM1	NBEA	NBN	NCOA3	NCOA6	NCOR2
NEFH	NF1	NF2	NFE2L2	NFKBIA	NFXL1	NIPBL	NKX2-1	NOTCH1	NOTCH2	NOTCH3	NPM1	NQO1	NR1H2	NRAS
NRP2	NSD1	NTRK1	NTRK2	NTRK3	NUP155	NUP93	OPRK1	OR11H4	OR2B11	OR52D1	OR5K4	OR6C76	OR8I2	ORAI1
PAK3	PALB2	PARK2	PAX5	PBRM1	PCDH12	PDCD1LG2	PDE11A	PDE7A	PDGFRA	PDGFRB	PDK1	PHGR1	PIK3C2B	PIK3C3
PIK3CA	PIK3CB	PIK3CG	PIK3R1	PIK3R2	PIP4K2A	PKD1L2	PLCG2	PMS2	POLD1	POLE	POLI	POTEC	PPP2R1A	PPP6C
PRDM1	PREX2	PRKAR1A	PRKCH	PRKCI	PRKDC	PRKRA	PROSER3	PRPF19	PRSS8	PRX	PTCH1	PTEN	PTGS2	PTPN11
QKI	RAC1	RAD50	RAD51	RAF1	RALY	RANBP2	RARA	RB1	RBM10	RBM27	RBM5	RET	RETNLB	RFX3
RGPD3	RGS12	RHPN2	RIC8A	RICTOR	RIN3	RNF145	RNF213	RNF43	ROCK1	ROS1	RP1L1	RPL8	RPS12	RPS9
RPTN	RPTOR	RRM1	RSBN1L	RUNX1	RUNX1T1	SCAI	SCYL2	SDHA	SDHB	SDHC	SDHD	SEC31A	SELE	SELPLG
SEMA3C	SEMA5B	SEPP1	SERPINA10	SETBP1	SETD2	SF3B1	SH3GL1	SI	SIK2	SKIDA1	SLAMF1	SLC11A2	SLC19A1	SLC22A2
SLC28A3	SLC29A1	SLC2A5	SLC35F5	SLC35G2	SLC36A2	SLC3A2	SLC6A18	SLCO1B3	SLIT2	SLK	SLX4	SMAD2	SMAD3	SMAD4
SMARCA4	SMARCB1	SMO	SNCAIP	SNX13	SOCS1	SOD2	SOX10	SOX11	SOX2	SOX9	SPATA3	SPEN	SPOP	SPTA1
SRBD1	SRC	SRD5A2	SRGAP3	SRPR	SRSF2	SSTR4	ST18	STAG2	STAT3	STAT4	STK11	STMN1	SUFU	SULT1A1
SVIL	SYK	TAF1	TAF1B	TBC1D23	TBK1	TBX3	TCERG1	TEAD2	TERC	TERT	TET2	TFAM	TGFBR2	THAP2
THAP3	THAP5	TMBIM4	TMEM106B	TMEM37	TMEM60	TMEM97	TNFAIP3	TNFAIP6	TNFRSF14	TOMM70	TOP1	TOP2A	TP53	TPMT
TRIM48	TRIM51	TRMT10C	TRRAP	TSC1	TSC2	TSHR	TTK	TTLL10	TVP23A	TXNDC2	TYMS	U2AF1	UBA7	UBE3C
UBE4A	UBR5	UGT1A1	UHRF1	ULK4	UMPS	UPF3A	USP35	USP36	VEGFA	VEZT	VHL	VIT	WDR37	WDR66
WDTC1	WISP3	WT1	XPC	XPO1	XRCC1	XRCC2	XYLT2	ZBTB2	ZFP37	ZFR2	ZNF217	ZNF365	ZNF429	ZNF462
ZNF479	ZNF516	ZNF527	ZNF605	ZNF703	ZNF717	ZNF776	ZNF814	ZNF844						
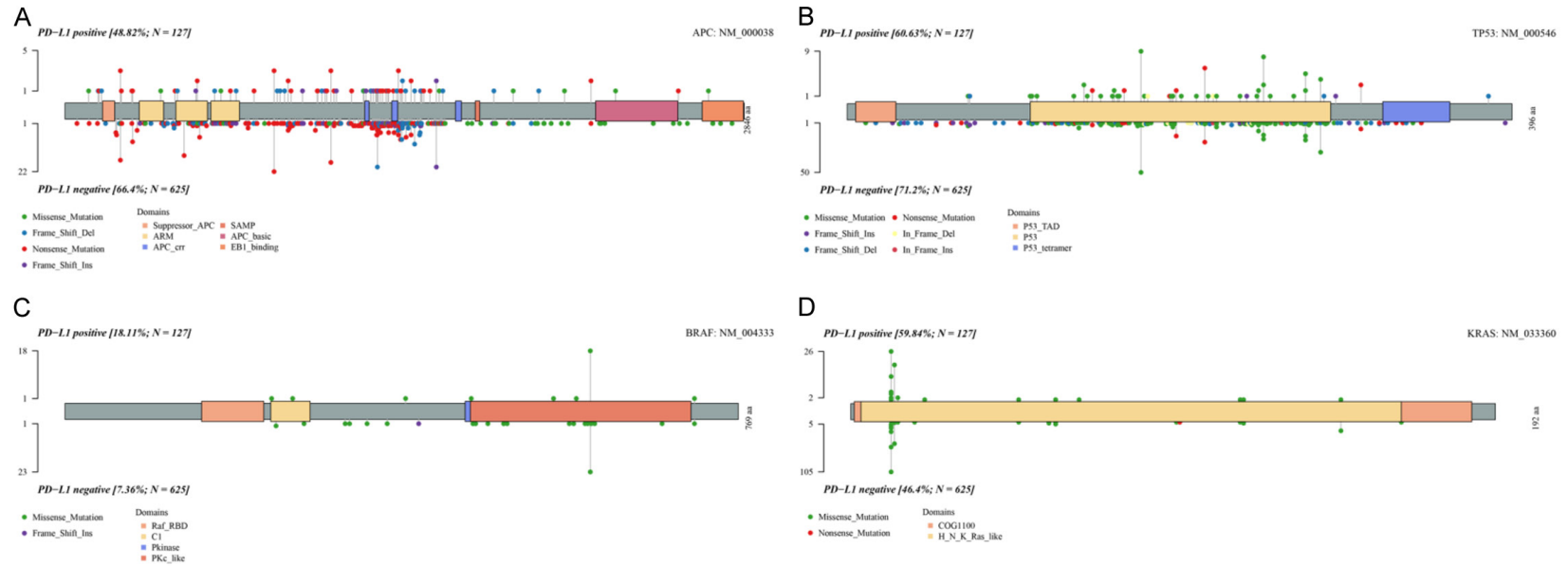
Figure S1. Genetic analysis of the difference in *APC* (A), *TP53* (B), *BRAF* (C), *KRAS* (D) mutation. Distribution of mutations and their position in the PD-L1 positive group and PD-L1 negative group.